Ultrasmall Graphene Oxide Supported Gold Nanoparticles as Adjuvants Improve Humoral and Cellular Immunity in Mice

Yuhua Cao, Yufei Ma, Mengxin Zhang, Haiming Wang, Xiaolong Tu, He Shen, Jianwu Dai, Huichen Guo, and Zhijun Zhang**

Adjuvants play an important role in vaccines. Alum and MF59 are two dominant kinds of adjuvants used in humans. Both of them, however, have limited capacity to generate the cellular immune response required for vaccines against cancers and viral diseases. It is desirable to develop new and efficient adjuvants with the aim of improving the cellular immune response against the antigen. Here, the feasibility and efficiency of ultrasmall graphene oxide supported gold nanoparticles (usGO-Au) as a new immune adjuvant to improve immune responses are explored. usGO-Au is obtained from reduction of chloroauric acid using usGO and then decorated with ovalbumin (OVA, a model antigen) through physical adsorption to construct usGO-Au@OVA. As the results show, the as-synthesized usGO-Au@OVA can efficiently stimulate RAW264.7 cells to secrete tumor necrosis factor-α (TNF-α), a mediator for cellular immune response. In vivo studies demonstrate that usGO-Au@OVA can also promote robust OVA specific antibody response, $CD8^+$ T cells proliferation, and different cytokines secretion. The results indicate that using usGO-Au as an adjuvant can stimulate potent humoral and cellular immune responses against antigens, which may promote better understanding of cellular immune response and facilitate potential applications for cancer and viral vaccines.

1. Introduction

Adjuvants are considered to be key components that are capable of enhancing and/or shaping antigen-specific immune responses in vaccines.[1] Currently, aluminum (alum) compound, MPL (monophosphoryl lipid A) and MF59 are the most extensively used adjuvants approved in clinical administration.[2,3] However, these conventional adjuvants have limited ability to promote sufficient cellular immune responses against cancer and intracellular pathogens, such as viruses.[4–8] Nanomaterials, on the other hand, are developed as potential vaccine carriers and adjuvants and have been extensively proven to effectively stimulate humoral and cellular immunity.[9,10] For example, α-Al_2O_3 nanoparticles, compared to conventional alum adjuvant, efficiently enhanced antigen cross-presentation and therefore improved the anticancer immune response;[9,11] polymeric nanoparticles efficiently delivered antigen into pulmonary dendritic cells, and released the antigen after endocytosis for optimal cross-presentation.[12] Fullerenol nanoparticles showed high loading capacity of HIV-1 DNA plasmid encoding the HIV-1 envelope protein gp145, and simultaneously stimulated strong cellular immune responses to the HIV DNA vaccine.[13] These studies demonstrated that nanomaterials can potentially play a number of roles in vaccination, such as enabling efficient antigen delivery and cross-presentation, reducing adjuvant dose, and translating the functionality of biologically derived materials to more robust platforms with improved shelf life and thermal stability.[12,14] Although these tentative efforts encourage the development of nanoparticle-based adjuvants, few studies on the clinic applications of nanomaterials as immune adjuvants are reported so far.

Y. Cao, Dr. Y. Ma, M. Zhang, H. Wang, X. Tu, H. Shen, Prof. J. Dai, Prof. Z. Zhang
CAS Key Laboratory for Nano-Bio Interface Research
Suzhou Key Laboratory for Nanotheranostics
Division of Nanobiomedicine
Suzhou Institute of Nano-Tech and Nano-Bionics
Chinese Academy of Sciences
Suzhou 215123, China
E-mail: zjzhang2007@sinano.ac.cn

Y. Cao, M. Zhang, X. Tu, H. Shen
University of Chinese Academy of Sciences
19 Yuquan Road, Beijing 100049, China

H. Wang, Prof. H. Guo
State Key Laboratory of Veterinary Etiological Biology
OIE/National Foot-and-Mouth Disease Reference Laboratory
Lanzhou Veterinary Research Institute
Chinese Academy of Agricultural Sciences
Lanzhou, Gansu 730046, China
E-mail: ghch-2004@hotmail.com

DOI: 10.1002/adfm.201401358

Gold nanoparticles (AuNPs) have been widely used in biomedicine because of their good biocompatibility, biological inertness, and facile preparation.[15–17] In addition, AuNPs have been reported to serve as vaccine carrier and adjuvant to deliver protein and DNA to induce potent humoral and cellular immune response without significant cytotoxicity.[18–22] Furthermore, naked spherical and cubic AuNPs could elicit dendritic cells to secrete TNF-α, IL-6, and IL-12 cytokines, which are crucial for regulation of cytotoxic T cell immune response.[23] However, AuNPs bind to antigens mainly through Au-S bond, which requires specific modification of the antigen and generally comes with low affinity, leading to insufficient antigen exposure and presentation and, consequently, deficient immune protection. Additionally, previous studies on using protein-AuNPs conjugates as adjuvant mainly focused on the induction of humoral immunity but not on cellular immunity. Therefore, it is urgent to improve the antigen-delivery capability of AuNPs and to investigate the cellular immunity of AuNPs-based nanomaterials in order to use them in clinical applications.

Graphene oxide (GO) is known for its excellent biocompatibility, high surface area, and extraordinary adsorbing ability, and thus it has attracted substantial attention in biomedical applications including drug, gene, and protein delivery.[24–27] Moreover, GO can be decorated with numerous inorganic nanomaterials, such as Au, Ag, Pd, Pt, MnO_2, and Fe_3O_4 nanoparticles, to achieve specific functions for applications in catalysis, as surface enhanced Raman scattering substrates, for removal of water pollutants, in magnetic resonance imaging, etc.[28–30] Little attention, however, has been paid to explore the feasibility of GO-based nanocomposites in immunity.

Here, we report the in situ growth of gold nanoparticles on ultrasmall graphene oxide (usGO) sheets through direct reduction of chloroauric acid, and the further use of thus-prepared usGO-Au composites as a new adjuvant for improving humoral and cellular immune responses (**Scheme 1**). In our strategy, excellent adsorbing capacity of graphene oxide can improve the binding capacity of usGO-supported AuNPs to OVA proteins. We then examined in vitro and in vivo immune competence of usGO-Au@OVA. The in vitro experiments include the cytokines secretion by RAW264.7 incubated with usGO-Au@OVA or OVA. For the in vivo experiments, the antibody generation and cytotoxic $CD8^+$ T cells proliferation against OVA protein was investigated in mice immunized with OVA, usGO-Au@OVA or Alum@OVA, and the cytokines secretion in the mice serum was also investigated. This study provides methods for the rational design of nanomaterials as a versatile platform for cellular immunity.

2. Results and Discussion

2.1. Preparation of usGO, usGO-Au, usGO-Au@OVA, OVA-FITC, and usGO-Au@OVA-FITC

The yellowish brown usGO sample was obtained with a production yield as high as 60%, and is highly soluble in phosphate buffered saline (PBS) and cell culture medium. Transmission electron microscopy (TEM) images of usGO (**Figure 1**a) show that the size of usGO varies from 3 to 5 nm, which is much smaller than that of GO synthesized using modified Hummer's method.[27] As Scheme 1a shows, AuNPs were in situ grown on the surfaces of usGO sheets without any other reagents, and then loaded with OVA through physical adsorption and Au-S bond.[21,24] AuNPs grown on usGO sheets, as characterized with TEM (Figure 1b), exhibit spherical shape within size range of 5–10 nm, and show an absorption peak at 530–540 nm in UV-vis spectrum (Figure 1c). usGO-Au@OVA possesses an absorption peak at 280 nm, suggesting the existence of aromatic

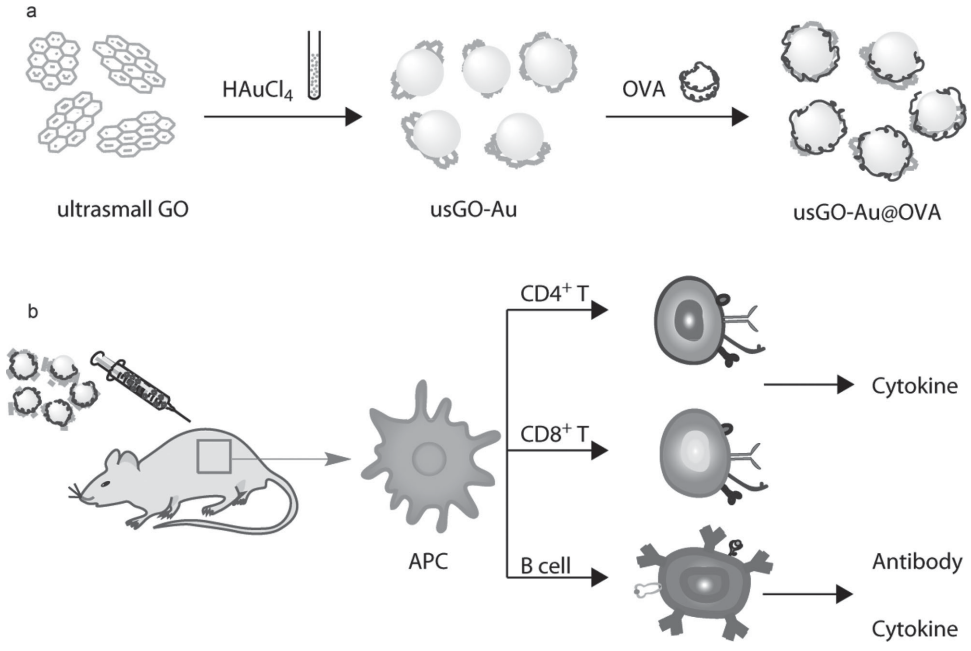

Scheme 1. Schematic illustration of a) preparation of usGO-Au@OVA vaccine and b) procedure for assessment of humoral and cellular immunity in vivo.

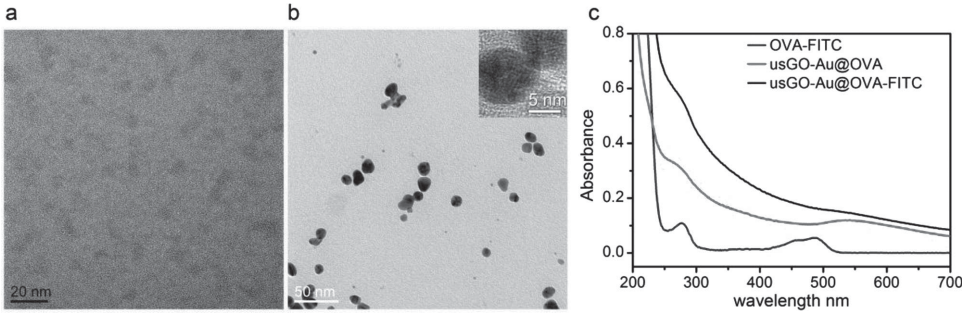

Figure 1. TEM images of a) usGO and b) usGO-Au@OVA. c) UV-vis spectra of OVA labled with FITC, OVA and OVA-FITC loaded on usGO-Au, respectively.

groups from the OVA. According to UV-Vis results, the OVA-loading capability of AuNPs is poor due to weak adsorption of the Au NPs to OVA, which was significantly improved through the formation of usGO-Au composites. In addition, the coupling of fluorescein isothiocyanate (FITC) with OVA, and further loading of OVA-FITC on usGO-Au are confirmed by the strong absorption peak in the UV-vis spectrum (Figure 1c) at around 488 nm, which corresponds to FITC.

2.2. MTT Assay and Cellular Uptake of usGO-Au@OVA

The biocompatibility of usGO-Au@OVA is a prerequisite for its biomedical applications as an adjuvant. 3-(4,5-Dimethylthiazol-2-yl)-2,5-diphenyltetrazolium bromide (MTT) assay (**Figure 2**a) indicates that no obvious toxicity in Hep G2 is observed after 48 h of incubation with usGO-Au@OVA, even at a concentration as high as 80 μg mL^{-1} of OVA, suggesting the good biocompatibility of usGO-Au@OVA.

To stimulate immune response, exogenous antigen needs to be ingested by antigen-presenting cells (APC), then processed and presented on the APC cell surface for lymphocytes recognition. The uptake of APC to antigen is crucial for antigen-presentation.[11,22] Confocal fluorescence microscopy was employed to monitor the cellular uptake efficiency of usGO-Au@OVA-FITC and OVA-FITC, after incubating the materials with RAW264.7 cells for 16 h. As shown in **Figure 3**, a strong fluorescence in the cells incubated with usGO-Au@OVA-FITC, in contrast to weak fluorescence in the cells with OVA-FITC (Figure 3), is observed, suggesting that usGO-Au facilitates the cellular uptake of OVA. These results are different to a report of Bastús and co-workers,[31] in which they found that a repetitive and homogenous antigens coated (rather than BSA-digested) AuNPs can be internalized by macrophages. Comparing with the report of Bastús, our result suggested that usGO may play an important role for the usGO-Au@OVA internalization.

2.3. Cytokine Secretion from RAW264.7 Cells

Tumor necrosis factor-α (TNF-α), a pro-inflammatory cytokine mainly produced by macrophages and Th1 subset of $CD4^+$ T cells, is one of the most important cytokines in cellular immunity. It can induce fever, cell apoptosis, and inflammation, and also inhibits tumorigenesis and viral replication. Previous study showed that unmethylated CpG motifs, which promoted potent cellular immune responses, induced the TNF-α secretion of RAW264.7 in vitro.[32] More importantly, CpG-conjugated AuNPs strongly enhanced the secretion of TNF-α after incubation with RAW264.7 cells.[22] To evaluate the capability of usGO-Au@OVA in promoting the cellular immunity, we tested the TNF-α level secreted by RAW264.7 cells after treatments with OVA-based materials at 10 or 1 μg mL^{-1} of OVA, respectively. We find that both OVA and usGO-Au@OVA can induce the

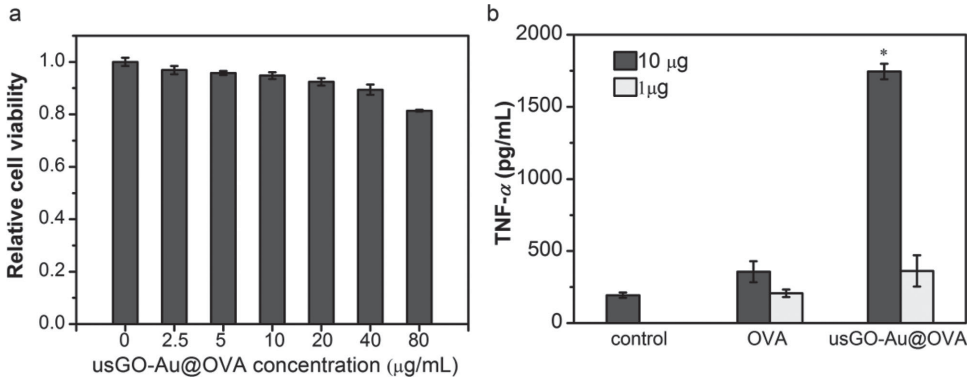

Figure 2. a) Cytotoxicity of usGO-Au@OVA to HepG2 and b) the TNF-α secretion by RAW264.7 incubated with usGO-Au@OVA and OVA. HepG2 cells were treated with usGO-Au@OVA at different concentrations for 48 h. The toxicity of usGO-Au@OVA to HepG2 was analyzed using MTT assay. RAW264.7 cells were treated with different materials for 8 h at the indicated concentrations. The concentrations of TNF-α in culture media were measured using an ELISA kit. The results were expressed as mean ± SD ($n = 3$). *$p < 0.05$ versus the cells treated with OVA or control.

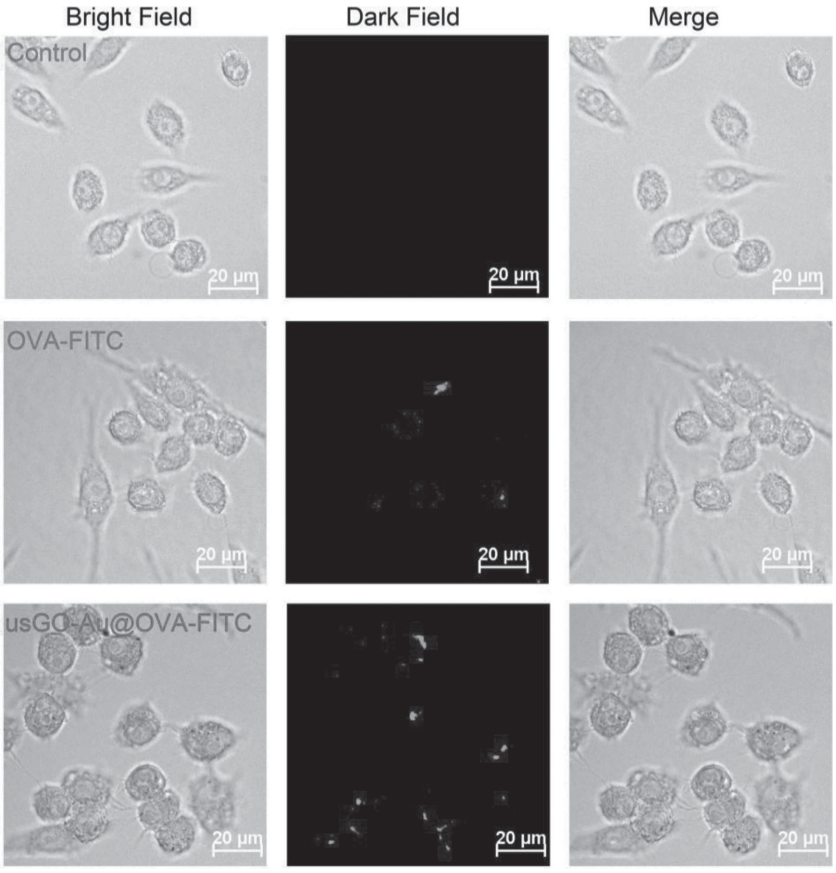

Figure 3. The cellular uptake of usGO-Au@OVA. Confocal fluorescence images of RAW264.7 cells incubated with usGO-Au@OVA-FITC and OVA-FITC for 16 h at 37 °C, respectively.

secretion of TNF-α in a dose-dependent manner (Figure 2b). Significantly, the amount of TNF-α stimulated by usGO-Au@OVA is approximately four-fold higher than that of naked OVA, suggesting that usGO-Au is critical for the immunostimulatory activity. Bastús et al. reported that AuNPs conjugated with repetitive and homogenous peptide antigens, but not with normal protein, induced an exacerbated TNF-α production.[31] Our results, however, demonstrated that nanocomposites of usGO-AuNPs and normal protein antigen can induce TNF-α secretion.

2.4. Antibody Titer

We further investigated whether usGO-Au@OVA could stimulate mouse antigen-specific humoral immune response. The mice were immunized with antigen via subcutaneous injection, and the serum was harvested at different time point post immunization. The anti-OVA antibody titer was measured using ELISA. For comparison, Alum@OVA was used as a positive control. One week after the last immunization, OVA-specific IgG is observed in all groups immunized with OVA-based materials (OVA, usGO-Au@OVA, and Alum@OVA). As **Figure 4**a shows, the anti-OVA antibody titer increases significantly in the usGO-Au@OVA (nearly 8 times, titer-1:30 000) and Alum@OVA groups (nearly 7 times, titer-1:60 000). Although the antibody titer induced by usGO-Au@OVA equals to Alum@OVA, the amount of AuNPs (5.85 μg) needed for sufficient OVA-loading (50 μg OVA) is much less than that of alum (285 μg). Furthermore, high levels of OVA-specific IgG are also observed on day 28 and 40 in mice immunized with usGO-Au@OVA (Figure 4b,c), and the antibody titer decreases with the time extension, as Figure 4 shows. All these results suggested that usGO-Au@OVA can promote potent humoral immune responses in mice.

2.5. Lymphocyte Viability and Proliferation Assay

The most important role of a vaccine is to facilitate the immune response of the organism occurring rapidly and strongly upon a second exposure to the same pathogen. We investigated the capability of T cell proliferation to understand the immune states of the organism indirectly. In this study, cell viability and proliferation were investigated using WST-1 assay. As shown in **Figure 5**a. OVA-based materials induce a dose-dependent proliferation, and higher cell viability compared with the negative control (saline). Moreover, the group immunized with usGO-Au@OVA exhibites the highest antigen-specific lymphocyte proliferation than the other groups. The CFSE staining was also employed for lymphocyte proliferation analysis. As shown in Figure 5b, the fluorescence intensity of CFSE in lymphocytes of groups immunized with OVA, Alum@OVA, and usGO-Au@OVA decreases compared to the negative control. The percentage of p3 area for OVA, Alum@OVA and usGO-Au@OVA are 31.2%, 40.5% and 47%, respectively, indicating a more efficient proliferation of lymphocyte in usGO-Au@OVA group than the other groups. These results suggested that usGO-Au@OVA can facilitate lymphocytes proliferation and maintain cells viability in an antigen-specific manner.

2.6. OVA-Specific $CD4^+$ T and $CD8^+$ T Cell Activation

The cell-mediated immunity can recognize and eliminate non-normal cells such as tumor cells or virus-infected cells. The activation of antigen specific $CD4^+$ T and $CD8^+$ CTLs (cytotoxic T lymphocytes) is a major feature of cell-mediated immune response. The activated $CD4^+$ T cells secrete many nonoverlapping sets of cytokines to mediate CTL and B cell functions.[33] $CD8^+$ CTLs have antigen-specific cytotoxic activity. They can eliminate foreign cells and alter self-cells by mounting a cytotoxic reaction that lyses their targets including allogeneic cells, malignant cells, and virus-infected cells.[34] In this experiment,

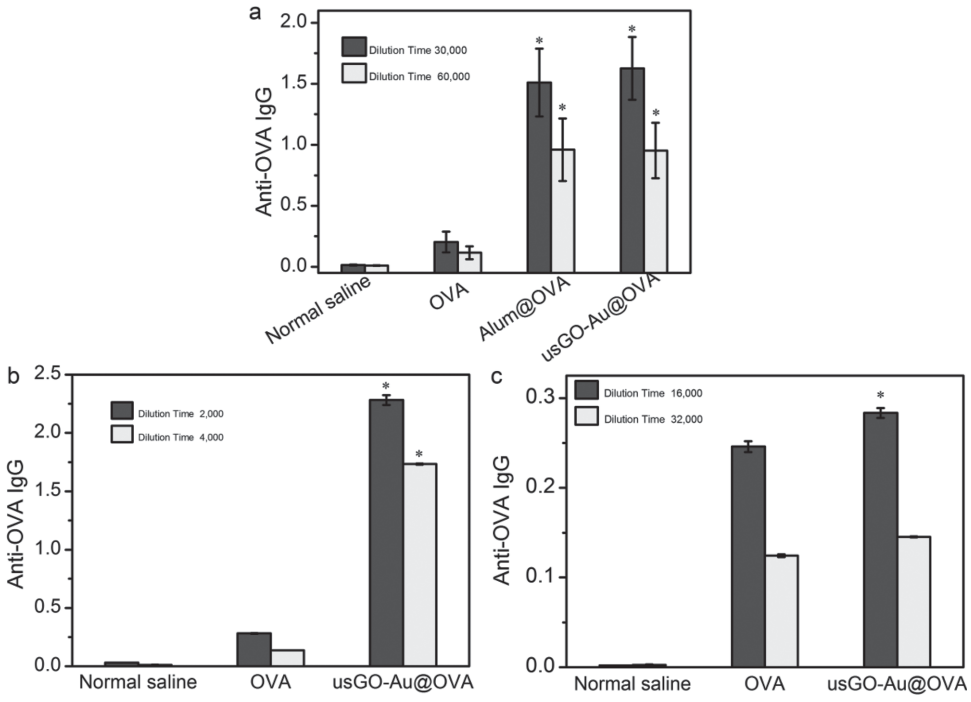

Figure 4. The anti-OVA antibody titer in mice serum immunized with 50 μg OVA based materials per mouse or normal saline. The mice were immunized three times at one week intervals (days 0, 7, 14) and sacrificed on days a) 21, b) 28, and c) 40 following the first immunization. The OVA antibody intensity in mice serum was measured using ELISA. $*p < 0.05$ versus the groups immunized with OVA or normal saline.

we tested whether the OVA-based vaccines could induce the activation of antigen-specific $CD4^+$ T and $CD8^+$ CTLs. Lymphocytes were isolated from spleens after three times of immunization, and then incubated with 10 μg mL^{-1} of OVA for 60 h. These cells were then stained with anti-CD3e-PE and anti-CD4-FITC or anti-CD8a-FITC antibodies. The cells were analyzed using FACS analysis. As shown in **Figure 6**, usGO-Au@OVA containing 25 μg OVA can stimulate $CD4^+$ T and $CD8^+$ CTLs proliferation, of which the level equals to that of naked OVA at 50 μg. Importantly, the amount of $CD4^+$ T cells and $CD8^+$ CTLs increases significantly in mice group immunized with usGO-Au@OVA (50 μg in terms of OVA) (**Figure 7**) compared with the group immunized with Alum@OVA (50 μg OVA), indicating that the $CD4^+$ T cells could proliferate to regulate the B cell and CTL activity after immunization with usGO-Au@OVA. Meanwhile, the $CD8^+$ T cells could also proliferate rapidly to eliminate the non-normal cells when the mice encountered the pathogen again.

2.7. IFN-γ, TNF-α, and IL-12 Secretion

IFN-γ plays a central role in many immunoregulatory processes, including the activation of mononuclear phagocytes and promoting the differentiation of fully CTLs from CD8 T cell precursors.[35] IFN-γ was mainly secreted by Th1 subset of $CD4^+$ T cells and $CD8^+$ CTLs to make the Th1 subset particularly suit to respond to viral infections and intracellular antigens such as tumor cells. In order to measure the level of IFN-γ in mouse serum, mice were immunized with normal saline, 50 μg OVA or 50 μg usGO-Au@OVA three times. The mice were sacrificed, and the serum was collected on day 40 after the first time immunization. The level of IFN-γ in serum was measured using ELISA. As shown in **Figure 8**b, the group immunized with usGO-Au@OVA shows notable increase of IFN-γ secretion in serum, while the group immunized with OVA exhibits a weak secretion of IFN-γ, which is slightly lower than that of the mice immunized with normal saline. These results demonstrate that naked protein antigen fail to stimulate a high level of IFN-γ secretion, in consistent with that reported by Lee et al.[21] Meanwhile, the immunization with usGO-Au@OVA leads to significant increase in the secretion of TNF-α, in good agreement with the in vitro experiments (Figure 2b and 8a). Furthermore, the levels of IL-12 were also determined in the serum of mice immunized with usGO-Au@OVA, OVA and normal saline, respectively, showing no detectable changes in these groups (Figure 8c). Our experiments demonstrate that usGO-Au exhibits ideal adjuvant activities to enhance cellular and humoral immunity.

3. Conclusion

We have developed usGO-Au nanocomposites as a new vaccine adjuvant to enhance humoral and cellular immune response. We find that usGO-Au@OVA can efficiently promote RAW264.7 cells to secrete TNF-α. In vivo study shows that usGO-Au@OVA can induce robust OVA specific antibody response, $CD4^+$ T and $CD8^+$ T cells proliferation, and the secretion of TNF-α and IFN-γ. The current work demonstrates that

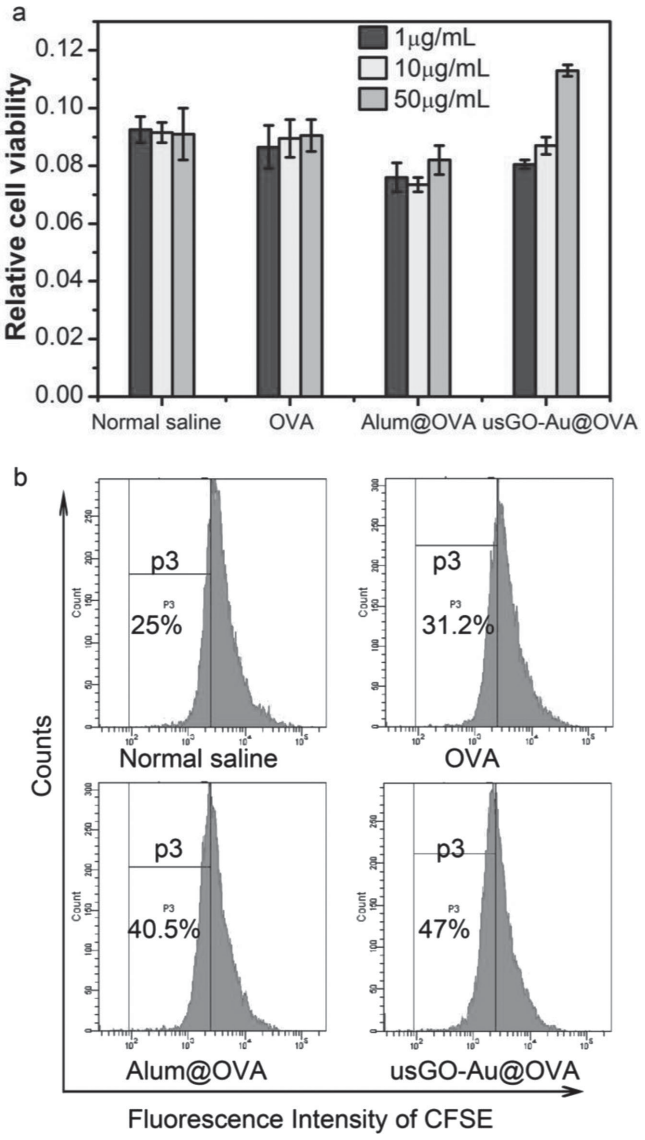

Figure 5. Lymphocytes viability and proliferation assay. a) The total lymphocytes were harvested from mouse spleens immunized with normal saline, 50 μg mL^{-1} OVA, Alum@OVA and usGO-Au@OVA respectively. Cells were then incubated with OVA for 48 h at 37 °C at different concentrations. The lymphocytes viability was analyzed using WST-1 assay. b) The lymphocytes proliferation capability was measured using flow cytometric analysis (FACS) analysis after incubated with 10 μg mL^{-1} OVA for 60 h.

the combination of usGO-Au with protein significantly improve humoral and cellular immune response, suggesting usGO-Au to be a good adjuvant candidate for cancer and viral vaccine.

4. Experimental Section

Materials and Instrumentation: Native graphite flake and FITC were purchased from Alfa Aesar and Sigma, respectively. OVA was obtained from Bio. Basic Inc. Other reagents were purchased from China National Medicine Corporation and used as received. UsGO and usGO-Au@OVA were characterized with a Tecnai G2 F20 S-Twin TEM and SHIMADZU UV-2550 spectrometer (UV-Vis spectrum). Fluorescence microscope images were captured on a laser confocal microscope (Nikon A1R). Cell lines were maintained in a water-jacketed CO_2 incubator (Thermo 3111). Results of MTT assay, WST-1 assay and ELISA were read out from a PerkinElmer 2030 multilabel reader. Data of lymphocyte proliferation, OVA-specific $CD4^+$ T and $CD8^+$ T cell activation were analyzed on BD FACSAria II flow cytometer.

Preparation of usGO: A yellowish black solution of usGO was obtained through a modified oxidative cutting method reported in previous reports.[36] In brief, graphite powder was cut into usGO in an oxidative mixture of H_2SO_4 and HNO_3 (V:V = 3:1) at 120 °C, following by neutralization of the mixture and further dialysis against deionized water. The concentration of final usGO solution was determined through measuring UV-vis absorbance at 230 nm.

Preparation of usGO-Au: $HAuCl_4$ (1.5 mg) was added into usGO (3 mg in 30 mL water), and the solution was stirred for 45 min at room temperature. The product was purified through dialysis against water overnight and then concentrated using a rotary evaporator. The concentration of usGO-Au was measured by UV-vis absorbance at 230 nm.

Preparation of OVA-FITC: OVA (10 mg) dissolved in sodium carbonate buffer (pH 9.8, 10 mL × 25 mM) was mixed with FITC (200 μL × 1mg mL^{-1}), and stirred at 4 °C overnight. The product was spin-dialyzed through 30 kDa cut-off filter (Millipore), and washed three times with 25 mM sodium carbonate and two times with water. The final solution was stored at –20 °C for future use.

Preparation of usGO-Au@OVA and usGO-Au@OVA-FITC: A mixture of usGO-Au (8 mg) with OVA or OVA-FITC (3 mg) was stirred at room temperature, collected by centrifugation (4000 rpm, 10 min), and washed (14000 rpm, 10 min) two times with water. After that, the precipitation was re-suspended in water, then sterilized using 0.22 μm membranes and stored at 4 °C for future use. The final product OVA-loaded usGO-Au was confirmed by UV-vis spectrum. The loading ratio of OVA on usGO-Au was determined using Bradford assay.

Cell Culture: The hepatocellular carcinoma cell line Hep G2 cells and mouse leukemic monocyte macrophage cell line RAW264.7 cells were purchased from Shanghai Institutes for Biological Sciences, Chinese Academy of Sciences and cultured at 37 °C in a 5% CO_2 atmosphere incubator in Dulbecco's modified Eagle's medium complemented with 10% fetal bovine serum (FBS, Hyclone) and 1% penicillin-streptomycin. For RAW264.7 cells culture, the FBS needs to be inactivated through heating at 56 °C for 30 min.

Cellular Uptake of usGO-Au@OVA-FITC and OVA-FITC: RAW264.7 cells were seeded into 36 mm cell dish at a density of 2×10^4 cells per well and maintained for 24 h. Then the cells were incubated with usGO-Au@OVA-FITC or OVA-FITC for 16 h. After that, the cells were washed twice with PBS to remove the residual materials, and fixed with 4% paraformaldehyde. Confocal fluorescence microscope was employed to probe the cellular uptake of usGO-Au@OVA-FITC or OVA-FITC.

Cytotoxicity Analysis: Cytotoxicity of usGO-Au@OVA was estimated using MTT assay. Hep G2 cells were seeded into 96-well plates at a density of 5×10^3 cells per well and maintained for 24 h. Next, the cells were incubated with usGO-Au@OVA at various concentrations for 48 h in DMEM containing 10% FBS. Relative cell viability was measured by standard MTT assay.

Cytokine Secretion of RAW264.7 Cells: RAW264.7 cells were seeded into 48-well plates at a density of 1.25×10^5 cells per well. After 24 h incubation, the cells were washed twice with 0.5 mL PBS and then incubated with usGO-Au@OVA or OVA at the concentration of 10 and 1μg mL^{-1} respectively for 8 h. The medium was collected and centrifuged at 2000 rpm for 10 min at 4 °C. The level of TNF-α secreted by RAW264.7 cells in medium was measured with a sandwich ELISA (enzyme-linked immunosorbent assay) method using a protocol recommended by the manufacturer (Boster, China).

Immunization: All animal experiments were conducted under protocols approved by the Soochow University Laboratory Animal Center. Healthy female C57BL/6 mice (Suzhou Industrial Park Animal Technology Co., Ltd.) at an average age of 6–7 weeks (18–22g) were housed in HEPA-filtered air and a constant climate (room temperature 23 ± 2 °C and relative humidity 40–70%) with a 12 h light/dark cycle with

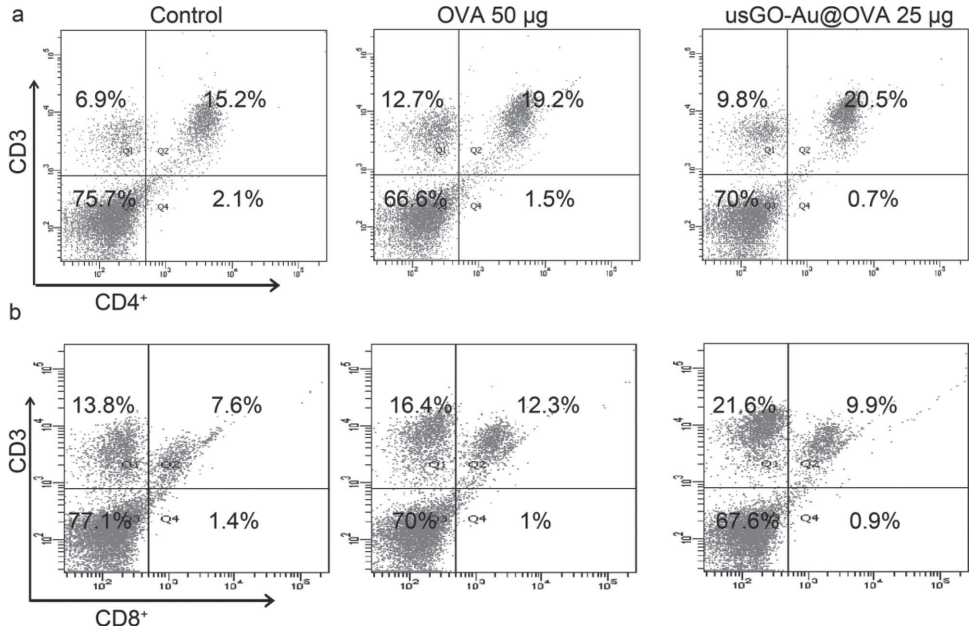

Figure 6. FACS analysis of a) $CD4^+$ and b) $CD8^+$ T cell populations after immunized with normal saline, 50 μg OVA, and 25 μg usGO-Au@OVA. The total lymphocytes were purified from immunized mouse spleens and then incubated with 10 μg mL^{-1} OVA for 60 h at 37 °C. The cells were then stained using anti-CD3e and anti-CD4 or anti-CD8a antibody.

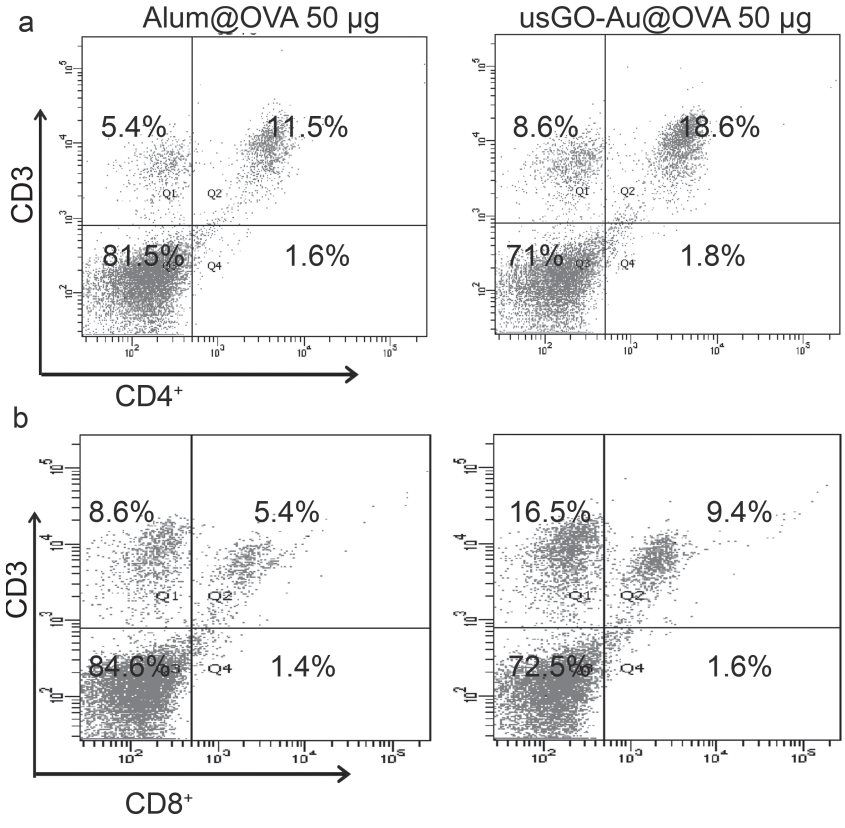

Figure 7. Comparison of the adjuvant effect between usGO-Au@OVA and Alum@OVA. The mice were immunized with usGO-Au@OVA and Alum@OVA. The percentage of a) $CD3^+$ $CD4^+$ and b) $CD3^+$ $CD8^+$ double positive cells were detected by FACS analysis.

free access to food and water. C57BL/6 mice were immunized with normal saline, OVA, OVA mixed with Alum (Alum@OVA), or usGO-Au@OVA three times on days 0, 7 and 14 by subcutaneous injection.

Lymphocyte Viability Assay: After two weeks following the final immunization, mice were sacrificed and the lymphocyte viability was evaluated using WST-1 assay. For WST-1 assay, lymphocytes were harvested from spleens of the various treatment groups mice immunized with normal saline, 50 μg OVA, 50 μg Alum@OVA (in terms of OVA), or 50 μg usGO-Au@OVA and then seeded into 96-well plates at a density of 1×10^6 cells/well. Then the cells were incubated with OVA at concentrations of 1, 10 and 50 μg mL^{-1} for 48 h, respectively. The lymphocyte viability was evaluated using WST-1 assay.

Lymphocyte Proliferation Assay: Lymphocyte proliferation was evaluated using CFDA SE staining. For CFSE staining, lymphocytes (1×10^6 cells) were isolated from groups of mice immunized with normal saline, 50 μg OVA, 50 μg Alum-OVA (in terms of OVA), or 50 μg usGO-Au@OVA after two weeks following the final immunization, and stained with CFDA SE for 10 min at 37 °C according to the protocol of the CFDA SE Cell Proliferation Assay and Tracking Kit (Beyotime Institute of Biotechnology). The cells were then washed twice with RPMI 1640 medium containing 10% FBS and seeded into 48-well plates before they were incubated with OVA at a concentration of 10 μg mL^{-1} for 60 h at 37 °C. The intensity of CFSE in the cells was analyzed using FACS.

Activation of $CD4^+$ T and $CD8^+$ T Cell: After two weeks following the final immunization, the

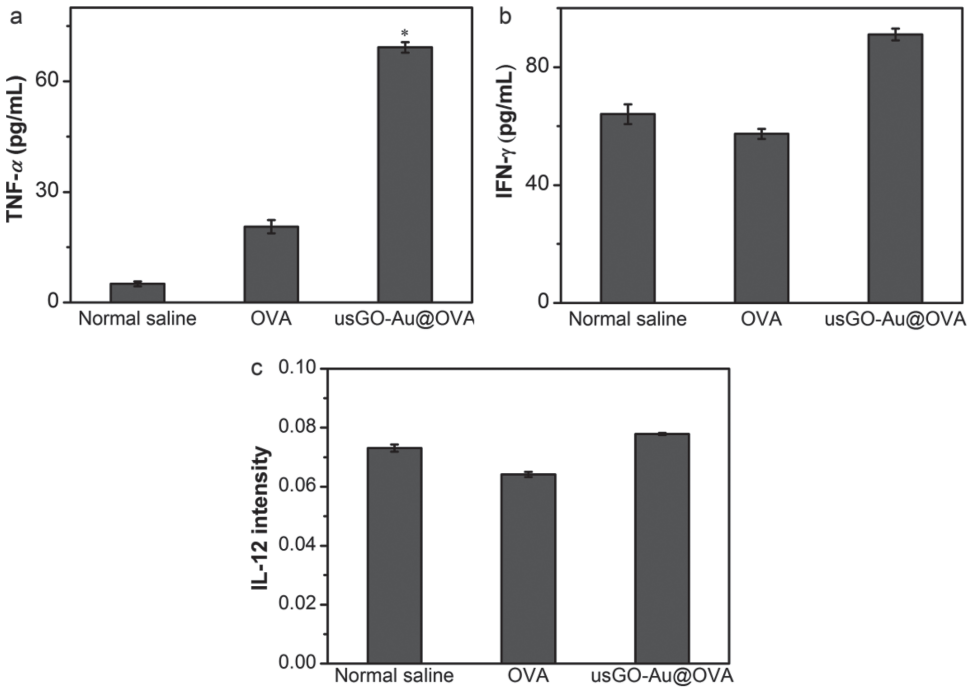

Figure 8. Cytokines secretion in mouse serum. The mice were immunized with normal saline, OVA, and usGO-Au@OVA, respectively. The a) TNF-α, b) INF-γ and c) IL-12 in serum were then measured using ELISA. *$p < 0.05$ versus the groups immunized with OVA or normal saline.

mice were sacrificed. Lymphocytes were harvested from the mice spleens and seeded into 48-well plates at a density of 1×10^6 cells/well before they were incubated with OVA (10 μg mL^{-1}) for 66 h. The cells were then stained with antibodies for surface markers, including anti-CD3e-PE, anti-CD8a-FITC and anti-CD4-FITC (BD) antibodies (all from BD Biosciences).The stained cells were analyzed using FACS analysis.

Levels of Anti-OVA Antibody, TNF-α, IFN-γ and IL-12: To evaluate the levels of anti-OVA antibody in the serum of mice from different groups, the mice were immunized on days 0, 7 and 14 and sacrificed on day 21, 28 and 40, respectively. The serum was collected. The levels of anti-OVA antibody in serum were determined using ELISA. To evaluate the levels of TNF-α, IFN-γ and IL-12 in mice serum, C57BL/6 mice were sacrificed on day 40. The levels of TNF-α, IFN-γ and IL-12 in serum were quantified using ELISA kit according to the protocol of the Mouse cytokine kit (Boster, China).

ELISA Measurement for the Titer of Anti-OVA Antibody: A 96-well ELISA plate was coated with 100 μL of 10 μg mL^{-1} OVA antigen in carbonate buffer (pH 9.6) at 4 °C overnight and then blocked with blocking buffer (TBS containing 1% BSA and 0.1% tween-20, pH 7.4) at 37 °C for 2 h. After washing with TBST (TBS containing 0.1% tween-20, pH 7.4), serially diluted mouse serum in buffer (TBS containing 0.1% BSA and 0.1% tween-20, pH 7.4) was added into wells and then incubated for 2 h at 37 °C. After washing with TBST, HRP-labeled anti-mouse IgG antibody (Beyotime Institute of Biotechnology) was added, and then incubated for another 1 h at 37 °C. The antibodies bound to OVA were detected using TMB substrate. To detect the anti-OVA antibody level in serum of mice sacrificed on day 21 and 40 after the first immunization, the ELISA plate was incubated with TMB for 10 min. For the serum of mice sacrificed on day 28, the incubation time is 5 min. The reaction was terminated by adding 2 M H_2SO_4, and then the absorbance at 450 nm was recorded using a multi-label reader.

Statistical Analysis: Data for cell viability, antibody and cytokines secretion assay were presented as mean ± SD and were statistically analyzed using the two-tailed Student's t test. $p < 0.05$ was considered to be significant.

Acknowledgements

Y.C. and Y.M. contributed equally to this work. The authors are grateful to the financial support from National Natural Science Foundation of China (No. 51361130033), the Ministry of Science and Technology of China (No. 2014CB965000), and by the State Key Laboratory of Veterinary Etiological Biology, Lanzhou Veterinary Research Institute, Chinese Academy of Agricultural Sciences (SKLVEB2013KFKT010).

Received: April 28, 2014
Revised: July 18, 2014
Published online: September 1, 2014

[1] S. G. Reed, M. T. Orr, C. B. Fox, *Nat. Med.* **2013**, *19*, 1597.
[2] T. C. Eickhoff, M. Myers, *Vaccine* **2002**, *20*, S1.
[3] G. Ott, G. L. Barchfeld, D. Chernoff, R. Radhakrishnan, P. van Hoogevest, G. Van Nest, *Pharm. Biotechnol.* **1995**, *6*, 277.
[4] R. L. Coffman, A. Sher, R. A. Seder, *Immunity* **2010**, *33*, 492.
[5] P. Marrack, A. S. McKee, M. W. Munks, *Nat. Rev. Immunol.* **2009**, *9*, 287.
[6] R. F. Pass, A.-M. Duliegè, S. Boppana, R. Sekulovich, S. Percell, W. Britt, R. L. Burke, *J. Infect. Dis.* **1999**, *180*, 970.
[7] P. Traquina, M. Morandi, M. Contorni, G. Van Nest, *J. Infect. Dis.* **1996**, *174*, 1168.
[8] J. O. Kahn, F. Sinangil, J. Baenziger, N. Murcar, D. Wynne, R. L. Coleman, K. S. Steimer, C. L. Dekker, D. Chernoff, *J. Infect. Dis.* **1994**, *170*, 1288.
[9] Z. Sun, W. Wang, R. Wang, J. Duan, Y. Hu, J. Ma, J. Zhou, S. Xie, X. Lu, Z. Zhu, *Cancer Nanotechnol.* **2010**, *1*, 63.
[10] M. Zaman, M. F. Good, I. Toth, *Methods* **2013**, *60*, 226.
[11] H. Y. Li, Y. H. Li, J. Jiao, H. M. Hu, *Nat. Nanotechnol.* **2011**, *6*, 645.
[12] C. Nembrini, A. Stano, K. Y. Dane, M. Ballester, A. J. van der Vlies, B. J. Marsland, M. A. Swartz, J. A. Hubbell, *Proc. Nat. Acad. Sci. USA* **2011**, *108*, E989.

[13] L. G. Xu, Y. Liu, Z. Y. Chen, W. Li, Y. Liu, L. M. Wang, L. Y. Ma, Y. M. Shao, Y. L. Zhao, C. Y. Chen, *Adv. Mater.* **2013**, *25*, 5928.
[14] J. A. Hubbell, S. N. Thomas, M. A. Swartz, *Nature* **2009**, *462*, 449.
[15] S. Rana, A. Bajaj, R. Mout, V. M. Rotello, *Adv. Drug Delivery Rev.* **2012**, *64*, 200.
[16] L. Dykman, N. Khlebtsov, *Chem. Soc. Rev.* **2012**, *41*, 2256.
[17] M. De, P. S. Ghosh, V. M. Rotello, *Adv. Mater.* **2008**, *20*, 4225.
[18] Y. S. Chen, Y. C. Hung, W. H. Lin, G. S. Huang, *Nanotechnology* **2010**, *21*, 195101.
[19] A. E. Gregory, E. D. Williamson, J. L. Prior, W. A. Butcher, I. J. Thompson, A. M. Shaw, R. W. Titball, *Vaccine* **2012**, *30*, 6777.
[20] Y. T. Wang, X. M. Lu, F. Zhu, P. Huang, Y. Yu, L. Zeng, Z. Y. Long, Y. M. Wu, *Biomaterials* **2011**, *32*, 7988.
[21] I. H. Lee, H. K. Kwon, S. An, D. Kim, S. Kim, M. K. Yu, J. H. Lee, T. S. Lee, S. H. Im, S. Jon, *Angew. Chem. Int. Ed.* **2012**, *51*, 8800.
[22] M. Wei, N. Chen, J. Li, M. Yin, L. Liang, Y. He, H. Y. Song, C. H. Fan, Q. Huang, *Angew. Chem. Int. Ed.* **2012**, *51*, 1202.
[23] K. Niikura, T. Matsunaga, T. Suzuki, S. Kobayashi, H. Yamaguchi, Y. Orba, A. Kawaguchi, H. Hasegawa, K. Kajino, T. Ninomiya, K. Ijiro, H. Sawa, *ACS Nano* **2013**, *7*, 3926.
[24] H. Shen, M. Liu, H. He, L. Zhang, J. Huang, Y. Chong, J. Dai, Z. Zhang, *ACS Appl. Mater. Interfaces* **2012**, *4*, 6317.
[25] Z. Liu, J. T. Robinson, X. Sun, H. Dai, *J. Am. Chem. Soc.* **2008**, *130*, 10876.
[26] L. Zhang, J. Xia, Q. Zhao, L. Liu, Z. Zhang, *Small* **2009**, *6*, 537.
[27] Y. H. Cao, Y. Chong, H. Shen, M. X. Zhang, J. Huang, Y. M. Zhu, Z. J. Zhang, *J. Mater. Chem. B* **2013**, *1*, 5602.
[28] J. Huang, C. Zong, H. Shen, Y. Cao, B. Ren, Z. Zhang, *Nanoscale* **2013**, *5*, 10591.
[29] J. Huang, C. Zong, H. Shen, M. Liu, B. Chen, B. Ren, Z. Zhang, *Small* **2012**, *8*, 2577.
[30] W. Chen, P. Yi, Y. Zhang, L. Zhang, Z. Deng, Z. Zhang, *ACS Appl. Mater. Interfaces* **2011**, *3*, 4085.
[31] N. G. Bastús, E. Sánchez-Tilló, S. Pujals, C. Farrera, C. López, E. Giralt, A. Celada, J. Lloberas, V. Puntes, *ACS Nano* **2009**, *3*, 1335.
[32] A. M. Krieg, *Annu. Rev. Immunol.* **2002**, *20*, 709.
[33] J. Zhu, W. E. Paul, *Blood* **2008**, *112*, 1557.
[34] J. T. Harty, A. R. Tvinnereim, D. W. White, *Annu. Rev. Immunol.* **2000**, *18*, 275.
[35] R. A. Goldsby, T. J. Kindt, B. A. Osborne, J. Kuby, *Immunology*, 5th edition, W. H. Freeman and Company, New York **2003**.
[36] J. Peng, W. Gao, B. K. Gupta, Z. Liu, R. Romero-Aburto, L. H. Ge, L. Song, L. B. Alemany, X. B. Zhan, G. H. Gao, S. A. Vithayathil, B. A. Kaipparettu, A. A. Marti, T. Hayashi, J. J. Zhu, P. M. Ajayan, *Nano Lett.* **2012**, *12*, 844.